Exponential stabilization of switched-reluctance motors via speed-sensorless feedback*

Antonio Loria Gerardo Espinosa–Pérez Erik Chumacero

Abstract

We solve the control problem of switched-reluctance motors without velocity measurements. Our controller is composed of a loop in the mechanical dynamics which consists of a PI^{2}D controller and a "tracking" controller closing an inner loop with the stator currents dynamics. The PI^{2}D controller consists in a linear proportional derivative controller in which the measurement of velocities is replaced by approximate derivatives of angular position. Then a double integrator is added, composed of an integral of the angular position errors and a second integral correction term in function of the approximate derivative. We show global exponential stability and illustrate the performance of our controller in numerical simulations.

Keywords: Switched-reluctance motor, PID control, nonlinear control.

I. Introduction

Switched-reluctance drives are typically very reliable and produce high torque at low speeds. This eliminates the use of gear boxes and makes them a suitable candidate for direct-drive applications. Nonetheless, the price paid for high performance is a technical difficulty –they are highly nonlinear electro-mechanical machines since the generated torque is a nonlinear function of stator currents and rotor position, and the magnetic saturation is required for its basic operation in order to maximize torque/mass radio.

In technological systems relying on electrical machines the necessity of eliminating the use of sensors for the mechanical variables (position and/or speed) is of special interest. This problem which is well known as *sensorless* control, is beyond the theoretical interest entailed by its difficulty –the requirement of not using mechanical sensors has its roots both in practical limitations and economic factors. On one hand, mechanical sensors exhibit undesirable behaviors in several scenarios such as high-noise sensitivity and reduced reliability. On the other, economic factors cannot be overestimated –the operation and implementation of this type of measurement devices may drastically increase the cost of a given setup.

There exist a large number of efficient heuristically-based and experimentally-validated control approaches to reduce the number of mechanical sensors in the loop –see *e.g.*, [1], [2], [3], [4], [5], [6], [7], [8]. However, to the best of the authors knowledge, articles on control of switched-reluctance drives that include a rigorous stability analysis, especially in a sensorless context, are rare. The main result in [9] establishes global asymptotic stability for a passivity-based controller in the case of unknown load however, it uses both mechanical variables, angular velocity and position measurements. A proportional-derivative-based controller is proposed in [10] but relying on

A Loria is with CNRS, E. Chumacero is with Univ Paris-Sud. Address: LSS-SUPELEC, 3 Rue Joliot Curie, Gif sur Yvette France. E-mail: loria@lss.supelec.fr. G. Espinosa is with FI – UNAM, A.P. 70-256, 04510 México D.F., MEXICO. gerardoe@unam.mx

the knowledge of the torque load. Other works on sensorless control and containing a theoretical analysis concern different electrical machines such as the induction motor –see *e.g.*, [11].

This paper is the outgrowth of [12], we exploit the physical characteristics of the nonlinear model of the switched-reluctance machine. The control design relies on the ability to separate the machine model into its electrical and mechanical components. Torque generation is achieved by following the "torque-sharing" approach of [10] with the aim of reducing the ripple in the mechanical variables that appears due to the electric commutation. A first control loop is designed to steer the stator currents to a desired "reference" that may be regarded as a virtual control input for the mechanical dynamics. Then, an "outer" control-loop is designed including a controller of proportional-integral-derivative type, probably the most often used in control practice. Specifically, we use the so-called PI^{2}D controller originally proposed in [13] for robot manipulators. The control law consists in a term proportional to the angular position error, a term which is proportional to an approximate derivative of the angular position, and two integrators: of angular position error and of the approximate derivative. We establish *global exponential* stability of the origin of the closed-loop via Lyapunov's direct method.

The rest of the paper is organized as follows. In the next section we present the motor model and explain the sharing-functions implementation approach. In Section III we present our main result and in Section IV we present a case-study in simulation, which reproduces a practically reasonable scenario. We close with some concluding remarks in Section V.

II. The motor model

It is well accepted that the three stator phases of a switched-reluctance motor may be assumed to be magnetically decoupled *i.e.*, the mutual inductance among stator phases is negligible. Under such hypothesis, a general three-phase dynamic model is given by

$$\dot{\psi}_j(\theta, i) + R i_j = u_j, \qquad j \in \{1,\ 2,\ 3\} \tag{1a}$$

$$J\dot{\omega} = T_e(\theta, i) - T_L(\theta, \omega) \tag{1b}$$

where for each phase j, u_j is the voltage applied to the stator terminals, i_j is the stator current and ψ_j is the flux linkage. R and J are physical parameters; the former accounts for the stator winding resistance and the latter denotes the total rotor inertia. The state variables are the angular velocity ω, and the angular rotor position θ, hence $\omega = \dot{\theta}$. The rotor dynamics is driven by the two inputs T_L which is the load torque and T_e which accounts for the mechanical torque of electrical origin. T_e depends both on the angular rotor position and on all the stator currents $i = [i_1,\ i_2,\ i_3]^\top$.

The flux linkage may be modeled in a number of ways as for instance the experimentally obtained and well-assimilated structure proposed in [14],

$$\psi_j(\theta, i) = \psi_s\Big(1 - \mathrm{e}^{-i_j f_j(\theta)}\Big), \quad i_j \geq 0 \tag{2}$$

where ψ_s is the saturated flux linkage and f_j which is known as the winding inductance, is strictly positive and periodic. Although Equation (2) accounts for magnetic saturation it leads to the definition of a non-invertible map for the generated torque $i \mapsto T_e$. Therefore, the inductance of each phase may be expressed as a strictly positive

Fourier series truncated at the first harmonic, $L_j(\theta)$ –see [14], [9]; this implies that $\psi_j(\theta, i) = L_j(\theta) i_j$ where

$$L_j(\theta) \;=\; l_0 - l_1 \cos\Big(N_r\theta - (j-1)\frac{2\pi}{3}\Big),$$

$l_0 > l_1 > 0$ and N_r is the number of rotor poles. Then, the dynamic model of the motor may be expressed as

$$u_j \;=\; L_j(\theta)\frac{di_j}{dt} + K_j(\theta)\omega i_j + Ri_j \tag{3a}$$

$$J\dot{\omega} \;=\; T_e(\theta, i) - T_L(\theta, \omega) \tag{3b}$$

where

$$K_j(\theta) = \frac{\partial L_j}{\partial \theta} = N_r l_1 \sin\Big(N_r\theta - (j-1)\frac{2\pi}{3}\Big)$$

corresponds to the phase-inductance variation relative to the rotor angular position. It is clear that

$$0 < l_m \le |L_j(\theta)| \le l_M, \quad |K_j(\theta)| \le k_M. \tag{4}$$

for some positive constants l_m, l_M and k_M.

Considering the decoupled behavior of stator windings, the mechanical torque T_e corresponds to the sum of torques T_j produced by each phase, that is

$$T_e = \sum_{j=1}^{3} T_j, \quad T_j = \frac{1}{2} K_j(\theta) i_j^2. \tag{5}$$

This model is adopted in both the electrical-machines and the control research communities –*cf.* [14].

The **speed-less control problem** for (3) is to design a dynamic controller with output $u = [u_1 \; u_2 \; u_3]^\top$ depending on the stator currents and rotor angular positions, such that $\omega(t)$ tracks any bounded smooth desired trajectory ω^*. Hence, the purpose is to avoid the use of speed sensors in the control scheme. This problem cannot be overestimated; from a control design viewpoint it is a crucial step towards full-sensorless control while from an implementation perspective, it eliminates the use of noisy velocity sensors. As mentioned in the introduction, speed-sensorless and full-sensorless have been addressed before however, never from an automatic-control perspective that is, without theoretical foundation.

III. Speed-less motor control

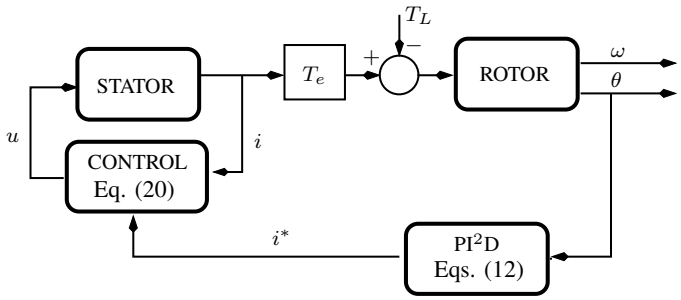

Fig. 1: Implementation of control scheme, composed of an outer rotor control loop and an inner stator control loop

The control approach consists in designing two controllers separately: the first closes an inner loop with the stator dynamics and is implemented using the input voltages that is, the actual control inputs. An outer control law, to

drive the rotor dynamics, is implemented using the mechanical torque of electrical origin as a virtual control input. The control implementation relies on the so-called sharing-torque technique –see Section III-A for a description and see Figure 1 for an illustration.

A. Torque delivery

Generally speaking, the control design starts with a given desired reference ω^*. Then, a $desired$ control input T_d is designed for the mechanical equation (3b) to steer $\omega \to \omega^*$. The control T_d must be implemented "through" the mechanical torque T_e that is, we define the reference mechanical torque T_e^* which satisfies

$$T_e^*(\theta, i^*) = \frac{1}{2}\Big(K_1(\theta)i_1^{*2} + K_2(\theta)i_2^{*2} + K_3(\theta)i_3^{*2}\Big) \tag{6}$$

where i_j^* is a current reference trajectory for each phase, which must be defined as a solution to

$$\frac{T_e^*}{J} = T_d \tag{7}$$

for any given T_d. That is, provided that $T_e = T_e^*$ the desired control torque JT_d acts upon the mechanical equation to drive $\omega \to \omega^*$. By ensuring an accurate current tracking that is, $i \to i^*$ it is guaranteed that $T_e \to T_e^*$ and consequently, that $\omega \to \omega^*$.

In order to solve (6) for i_j^*, we exploit the physics of the $switched$ reluctance motor. Note that the torque sign is only determined by the variation of the inductance that is, $T_j > 0$ if and only if $K_j > 0$ and $K_j = 0$ implies that no torque is produced 'through' the phase j –see Equation (5). Then, using ideas reported in [14] and [10] we introduce the following smooth current-switching policy. Define the sets

$$\Theta_j^+ = \{\theta \in [-\pi, \pi] : K_j(\theta) \geq 0\}$$
$$\Theta_j^- = \{\theta \in [-\pi, \pi] : K_j(\theta) < 0\}$$

where the superscripts $^+$ and $^-$ stand for required positive and negative torques respectively. Accordingly, let us introduce

$$m_j^+(\theta) > 0,\ \sum_{j=1}^{3} m_j^+(\theta) = 1 \quad \forall \theta \in \Theta^+,$$
$$m_j^-(\theta) > 0,\ \sum_{j=1}^{3} m_j^-(\theta) = 1 \quad \forall \theta \in \Theta^-$$

and given T_d, define

$$m_j(\theta) = \begin{cases} m_j^+(\theta) & \text{if} \quad T_d \geq 0, \\ m_j^-(\theta) & \text{if} \quad T_d < 0. \end{cases} \tag{8}$$

Then, we define the reference currents for $j \in \{1,\ 2,\ 3\}$ as

$$i_j^* = \begin{cases} \left[\dfrac{2Jm_j(\theta)T_d}{K_j(\theta)}\right]^{1/2} & \text{if } |K_j(\theta)| \neq 0 \\ 0 & \text{otherwise.} \end{cases} \tag{9}$$

The definition of $m_j(\theta)$ ensures that i_j^* exists for any θ and T_d. That is, depending on the current phase of the motor, the function $m_j(\theta)$ ensures that the respective signs of the numerator and of the denominator in the previous expression are equal for *at least one* $j \in \{1, 2, 3\}$ and the denominator $\sin\left(\theta - (j-1)\dfrac{2\pi}{3}\right) \neq 0$. Furthermore, for

implementation purposes hysteresis is typically introduced in the definition of i_j^* –see Eq. (9) to smoothly avoid the singularity at the points θ in the neighbourhood of $\{K_j(\theta) = 0\}$. In addition, it is imposed that $m_1 + m_2 + m_3 \equiv 1$ so by construction,

$$T_d = m_1(\theta)T_d + m_2(\theta)T_d + m_3(\theta)T_d.$$

Thus, roughly speaking the virtual control T_d is induced into the mechanical dynamics through a different reference, depending on the current phase. The transition is ensured by a proper definition of the functions m_j –*cf.* [9]. See also Section IV for a case-study.

B. Control of the rotor dynamics

The rotor controller that produces T_d is of the proportional-integral-derivative type, possibly the most popular controller in practice. It is reminiscent of the Proportional-Derivative-plus-load-compensation controller presented in [14] where the sharing-functions approach was proposed. However, we relax the assumption that the torque-load is known and that velocity is measured. Our main result extends previous work using both mechanical velocity and position measurements as in [9] as well as [10]. In contrast with available sensorless *ad hoc* controllers proposed without theoretical foundation, we establish global exponential stability hence robustness with respect to external disturbances, neglected dynamics, *etc.*

For control purposes, we view the rotor dynamics equation (1b), as a drift-less system perturbed by the input T_L. Its complexity comes from the fact that it is non-affine in the (virtual control) inputs i; such difficulty is overcome by using the torque-sharing technique described previously. Then, for a given reference ω^* and defining $e_\omega = \omega - \omega^*$, Equation (3b) may be equivalently written as

$$\dot{e}_\omega = T_d - \frac{T_L}{J} + \frac{T_e}{J} - \frac{T_e^*}{J} - \dot{\omega}^* \tag{10}$$

and the control problem comes to designing a control law T_d to stabilize the origin $\{e_\omega = 0\}$ of (10). Such controller must compensate for the constant perturbation T_L/J and be robust to the "disturbance" $T_e - T_e^*$ which vanishes by design. The former is compensated for by integral action; the latter, which accounts for the difference between the ideal mechanical torque T_e^*/J that stabilizes the system and the actual mechanical torque which depends on the stator currents, vanishes provided that the external control loop achieves current tracking. Indeed, this difference satisfies

$$|T_e - T_e^*| \leq \frac{k_M}{2}\left[|e_i|^2 + 2\,|i^*|\,|e_i|\right], \tag{11}$$

since T_e and T_e^* are quadratic functions uniformly bounded in θ.

For the rotor control law T_d, we chose to use the PI^{2}D controller introduced in [13] for robot manipulators. Its name comes from the fact that it corresponds to a modified PID controller; it consists in a correction term proportional to the tracking errors e_θ, a 'derivative' term proportional to filtered velocities ϑ and a double integral action, both on e_θ and ϑ. The choice of this controller is motivated by its mathematical simplicity and its physical properties: it is a linear controller which conserves the passivity properties of Lagrangian systems and ensures asymptotic stability, provided a property of detectability holds –see [15].

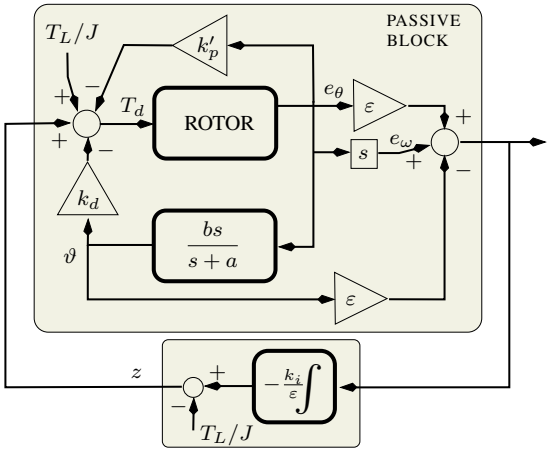

Fig. 2: For analysis purpose note that the rotor dynamics in closed loop forms a passive systems interconnection. The control implementation is illustrated in Figure 1.

The PI^{2}D controller for the rotor dynamics is defined by

$$T_d = -k_p e_\theta - k_d \vartheta + \nu + \dot{\omega}^* \tag{12a}$$

$$\dot{\nu} = -k_i(e_\theta - \vartheta) \tag{12b}$$

$$\dot{q}_c = -a(q_c + b e_\theta) \tag{12c}$$

$$\vartheta = q_c + b e_\theta \tag{12d}$$

where k_p, k_i, k_d, a, b are positive constants and we use the tracking errors $e_\omega = \omega - \omega^*$ and $e_\theta = \theta - \theta^*$ where

$$\theta^*(t) = \int_0^t \omega^*(s)ds, \quad \theta^*(0) = \theta_0^* \in [-\pi, \pi].$$

Note that since the variable to be controlled is ω, the initial value of $\theta^*(t)$ is innocuous. As usual, the integral gain k_i is chosen 'small' consequently, the estimation error of the load torque $\tilde{\nu}$ converges slowly to zero; this is not a drawback since the variable of interest is the angular velocity ω.

The last two equations in (12) correspond to the well-known and widely used 'dirty derivatives' or 'approximate differentiation'. The nicknames come from the observation that they are equivalent to

$$\vartheta = \frac{b}{s+a} e_\omega$$

where s is the Laplace variable. That is, ϑ is not an estimate of the velocities e_ω but a filtered version of it. In the limit case, when the pole is at $-\infty$, $\vartheta = e_\omega$ modulo the DC gain b/a.

One of the most attractive features of the controller (12) is that as for robot manipulators –see [15], the system (10) in closed loop with (12) may be regarded as the feedback interconnection of two passive systems; see Figure 2. The first passive block (shadowed in the figure) is defined by the map $z \mapsto \varepsilon[\mathrm{e}_\theta - \vartheta] + e_\omega$ where

$$z = \nu - \frac{T_L}{J} - \frac{k_i}{\varepsilon} e_\theta \tag{13}$$

and $\varepsilon > k_i$ is a small positive parameter. The second passive block is a simple integrator.

The rotor closed-loop dynamics, which corresponds to the feedback interconnection showed in Figure 2 is obtained by substituting (12a) and (13) into (10) and by differentiating on both sides of (12d) and (13), to obtain

$$\dot{e}_\theta = e_\omega \tag{14a}$$
$$\dot{e}_\omega = -k_d\vartheta - k'_p e_\theta + z + \frac{1}{J}\left(T_e - T_e^*\right) \tag{14b}$$
$$\dot{\vartheta} = -a\vartheta + be_\omega \tag{14c}$$
$$\dot{z} = -k_i(e_\theta - \vartheta) - \frac{k_i}{\varepsilon}e_\omega \tag{14d}$$

where $k'_p := k_p - k_i/\varepsilon$, $k_i \leq \varepsilon$. Note that we have added the input $\left(T_e - T_e^*\right)$ that comes from the stator dynamics although this is not represented in Figure 2. This input vanishes provided that the stator controller performs a perfect current tracking; this is better seen from the structure of (14) which may be rewritten in the clearer form

$$\begin{bmatrix} \dot{e}_\theta \\ \dot{e}_\omega \\ \dot{\vartheta} \\ \dot{z} \end{bmatrix} = \underbrace{\begin{bmatrix} 0 & 1 & 0 & 0 \\ -k'_p & 0 & -k_d & 1 \\ 0 & b & -a & 0 \\ -k_i & -k_i/\varepsilon & k_i & 0 \end{bmatrix}}_{A} \underbrace{\begin{bmatrix} e_\theta \\ e_\omega \\ \vartheta \\ z \end{bmatrix}}_{\zeta_1} + \underbrace{\begin{bmatrix} 0 \\ 1/J \\ 0 \\ 0 \end{bmatrix}}_{B} \left(T_e - T_e^*\right).$$

Note that the only nonlinearity corresponds to the additive input term $\left(T_e - T_e^*\right)$ and on the other hand, for appropriate values of the control gains, one can render the matrix A Hurwitz. Therefore, the system may be made input to state stable with respect to the input $\left(T_e - T_e^*\right)$ and asymptotic stability follows if $T_e - T_e^*$ tends to zero; this is the job of the stator controller, which we present next.

C. Control of the stator dynamics

The controller (12) stabilizes (the origin of) (10) exponentially, provided that perfect current tracking is achieved. Therefore, an inner control loop is added to steer $e_i = i - i^*$ to zero. This task may be achieved with the model-based nonlinear tracking controller

$$u^* = L(\theta)\frac{di^*}{dt} + K(\theta)\omega^* i + Ri^* - k_{px}e_i, \qquad k_{px} > 0 \tag{15}$$

where for convenience, we introduced $L(\theta) = \text{diag}\{L_j(\theta)\}$ and $K(\theta) = \text{diag}\{K_j(\theta)\}$.

The motivation to use this controller relies on the fact that it stabilizes the stator dynamics, robustly with respect to additive disturbances. This may be clear from the expression of the closed-loop dynamics (3), (15) to which we add an external input v, that is

$$\dot{e}_i = L(\theta)^{-1}[-(R + k_{px})e_i - K(\theta)ie_\omega] + v. \tag{16}$$

To see that the origin of the 'nominal' system $\dot{e}_i = -L(\theta)^{-1}(R + k_{px})e_i$ is exponentially stable, it suffices to invoke Lyapunov's direct method with the Lyapunov function

$$V_2(e_i) = \frac{1}{2}\left|e_i\right|^2,$$

whose total time derivative along the trajectories of the nominal system yields

$$\dot{V}_2 = -(R + k_{px})e_i^\top L^{-1}e_i \leq -\frac{1}{l_M}(R + k_{px})\left|e_i\right|^2$$

where for the last inequality, we used (4).

Exponential stability implies robustness with respect to disturbances, more precisely, local input to state stability. To make this property global, we chose the control gain k_{px} as a function of the measured states. To that end, note that

$$\left|L(\theta)^{-1}[-K(\theta)ie_\omega]\right| \leq \frac{k_M}{l_m}\Big(|e_\omega|\,|i| \Big),$$

so the total derivative of V_2 along the trajectories of the 'perturbed' system (16), yields

$$\dot{V}_2 \leq -\Big(\frac{R+k_{px}}{l_M} - \frac{k_M}{2l_m}\,|i|^2\Big)\,|e_i|^2 + v^\top e_i + \frac{k_M}{2l_m}e_\omega^2. \tag{17}$$

Hence, it suffices to make k_{px} dependent on the measured stator currents i, to render the factor of $|e_i|^2$ negative. Under this condition and in the case of perfect rotor velocity tracking ($e_\omega = 0$), the map $v \mapsto e_i$ is output strictly passive. Note also that the system is input to state stable with respect to the input $v + e_\omega$.

Although the control law (15) renders the stator dynamics robustly stable, note that the column vector $\frac{di^*}{dt} = \frac{d}{dt}[i_1^*\ i_2^*\ i_3^*]^\top$ depends on $\dot{T}_d$ where T_d is defined in (12a) hence, also on the unmeasurable error e_ω. That is,

$$\frac{di_j^*}{dt} = \begin{cases} \alpha_j[\rho_j + \delta_j e_\omega] & \text{if } |K_j(\theta)| \neq 0 \\ 0 & \text{otherwise.} \end{cases} \tag{18}$$

where

$$\alpha_j = \left(\frac{2Jm_jT_d}{K_j}\right)^{-\frac{1}{2}}, \tag{19a}$$

$$\rho_j = \frac{J}{K_j}\left(\beta_j + m_j'\omega^*T_d\right), \tag{19b}$$

$$\beta_j = m_j\left(k_{id}\vartheta - k_ie_\theta + \ddot{\omega}^* - \frac{T_dK_j'\omega^*}{K_j}\right), \tag{19c}$$

$$\delta_j = \frac{J}{K_j}\left(m_j'T_d - m_j\left(k_{pd} + \frac{T_dK_j'}{K_j}\right)\right), \tag{19d}$$

$k_{id} = k_i + ak_d$, $k_{pd} = k_p + bk_d$, $m_j' = \dfrac{\partial m_j}{\partial\theta}$ and $K_j' = \dfrac{\partial K_j}{\partial\theta}$. Since it is assumed that e_ω is not measured, only the terms α =diag$\{\alpha_j\}$ and $\rho = [\rho_1\ , \rho_2\ , \rho_3]^\top$ may be implemented in the control law. Therefore, we use the control law

$$u = L(\theta)\alpha\rho + K(\theta)\omega^*i + Ri^* - k_{px}e_i \tag{20}$$

which satisfies $u = u^* - L(\theta)\alpha\delta e_\omega$ where $\delta = [\delta_1\ \delta_2\ \delta_3]^\top$. With this modification, the closed-loop dynamics takes the form (16) with $v = \alpha\delta e_\omega$. Therefore, after (17) and the triangle inequality, the total derivative of V_2 along the closed-loop trajectories of (3a), (20) yields

$$\dot{V}_2 \leq -\Big(\frac{R+k_{px}}{l_M} - \frac{k_M}{2l_m}|i|^2 - \frac{1}{2}\,|\alpha\delta|^2\Big)\,|e_i|^2 + \frac{1}{2}\Big(\frac{k_M}{l_m} + 1\Big)\,|e_\omega|^2 \tag{21}$$

that is, for an adequate choice of k_{px} the factor of $|e_i|^2$ is negative and the system is input to state stable with respect to the input e_ω.

D. Main result

We are ready to present our main result: global exponential stabilization of the switched-reluctance motor without velocity measurements. The result relies on the fact that the rotor dynamics in closed-loop with the PI^{2}D controller is input to state stable with respect to the input e_i while the stator dynamics in closed loop with the control law (20) is input to state stable with respect to the input e_ω.

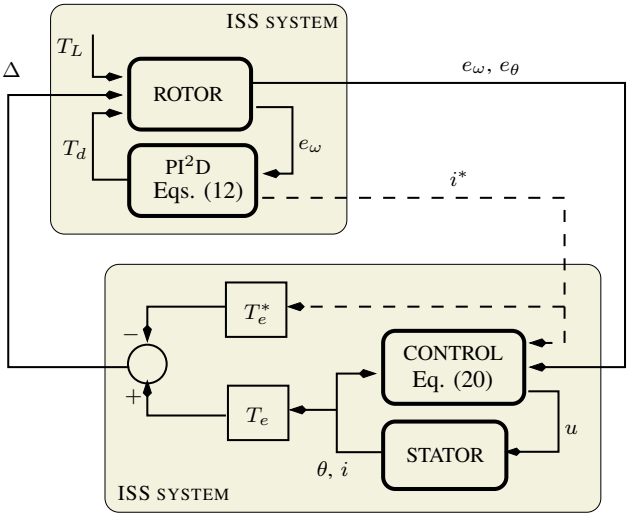

Fig. 3: Analysis: the closed-loop system consists in two ISS controlled sub-systems

Proposition 1: Consider the system (3) in closed loop with the controller (12), (19), (20). Let k'_{px}, $\gamma_1 > 0$, $\lambda \in (0,1)$,

$$k_d > \frac{3b}{b-1}\left[\frac{k_M}{l_m}+1\right], \qquad k_d < \frac{3a}{2}\frac{\lambda}{\lambda+1} \tag{22}$$

$$b \geq 2a+1, \qquad k'_p > k_d \tag{23}$$

$$k_{px} := k'_{px} + \frac{l_M}{2}\left[\frac{k_M}{l_m}|i|^2 + |\alpha\delta|^2 + \frac{\gamma_1 k_M l_m}{2}\left(\frac{|e_i|^2}{\mu_2} + \frac{4\,|i^*|^2}{\mu_1}\right)\right]. \tag{24}$$

Then, the origin of the closed-loop system is globally exponentially stable.

The conditions of the proposition hold if the control gains are chosen as follows: 1) define $c = k_M/l_m + 1$ and let $k_d \approx 3c$ but satisfying $k_d > 3c$; 2) pick $\lambda \in (0,1)$ and define $k'_p := k_d/\lambda$; 3) choose a such that the second inequality in (22) holds; 4) define b such that $b \geq 2a+1$ and verify that $k_d > 3bc/(b-1)$; if necessary, redefine k_d so as to satisfy the latter.

The proof of Proposition 1 is based on Lyapunov's direct method and the previous developments. Define $\zeta_1 = [e_\theta\, e_\omega\, \vartheta\, z]^\top$ then we write (14) as $\dot{\zeta}_1 = A\zeta_1 + B(T_e - T_e^*)$. Let $\varepsilon_1 = \varepsilon > k_i$ and ε_2 be two "small" positive numbers and consider the Lyapunov function $V_1(\zeta_1) = \frac{1}{2}\zeta_1^\top P \zeta_1$ with

$$P = \begin{bmatrix} k'_p & \varepsilon_1 & 0 & 0 \\ \varepsilon_1 & 1 & -\varepsilon_1 & -\varepsilon_2 \\ 0 & -\varepsilon_1 & k_d/b & 0 \\ 0 & -\varepsilon_2 & 0 & \varepsilon_1/k_i \end{bmatrix}.$$

This matrix is diagonal dominant, hence positive definite, if

$$k_p' > \varepsilon_1, \quad 1 > 2\varepsilon_1 + \varepsilon_2$$
$$\frac{k_d}{b} > \varepsilon_1 \quad \frac{\varepsilon_1}{k_i} > \varepsilon_2$$

which hold for sufficiently small k_i, ε_1 and ε_2. Also, we have

$$-\frac{1}{2}(A^\top P + PA) =$$
$$\underbrace{\frac{1}{2}\begin{bmatrix} \varepsilon_1 k_p' & -\varepsilon_2 k_i & \varepsilon_1(k_d - k_p') & 0 \\ -\varepsilon_2 k_i & \varepsilon_1(b-1) - 2\dfrac{\varepsilon_2 k_i}{\varepsilon_1} & \varepsilon_2 k_i - \varepsilon_1 a & 0 \\ \varepsilon_1(k_d - k_p') & \varepsilon_2 k_i - \varepsilon_1 a & k_d\Big(\dfrac{a}{b} - \varepsilon_1\Big) & 0 \\ 0 & 0 & 0 & \varepsilon_2 \end{bmatrix}}_{Q_1} +$$
$$\underbrace{\frac{1}{2}\begin{bmatrix} \varepsilon_1 k_p' & 0 & 0 & -\varepsilon_2 k_p' \\ 0 & \varepsilon_1(b-1) & 0 & 0 \\ 0 & 0 & k_d\Big(\dfrac{a}{b} - \varepsilon_1\Big) & -k_d\varepsilon_2 \\ -\varepsilon_2 k_p' & 0 & -k_d\varepsilon_2 & \varepsilon_2 \end{bmatrix}}_{Q_2} \tag{25}$$

The matrix Q_1 in (25) is positive definite if each element in its main diagonal is positive and the matrix is diagonal dominant. This holds for small values of ε_1 and ε_2 and control gains satisfying (23). The matrix Q_2 is positive semidefinite for sufficiently small values of ε_1 and ε_2; indeed, $-\zeta_1^\top Q_2 \zeta_1 \leq -(1/2)\varepsilon_1(b-1)e_\omega^2$. See Appendix VI-A for details. We conclude that

$$-\frac{1}{2}(A^\top P + PA) = Q, \quad Q = Q^\top > 0$$

and the total time derivative of $V_1(\zeta_1)$ yields

$$\dot{V}_1 = -\zeta_1^\top Q \zeta_1 + \zeta_1^\top PB(T_e - T_e^*).$$

To prove input-to-state stability with input e_i let q_m be the smallest eigenvalue of Q_1 and let $\gamma_1 \geq |PB|$ then,

$$\dot{V}_1 \leq -q_m |\zeta_1|^2 + \gamma_1 |\zeta_1| |T_e - T_e^*|.$$

Next, we use (11) to obtain

$$\begin{aligned} \dot{V}_1 &\leq -q_m |\zeta_1|^2 + \frac{\gamma_1 k_M}{2} |\zeta_1| \left[|e_i|^2 + 2|i^*||e_i| \right] + \frac{\gamma_1 k_M}{4} \left[\frac{4|i^*|^2 |e_i|^2}{\mu_1} + \mu_1 |\zeta_1|^2 \right] \\ &\leq -\left[q_m - \frac{\gamma_1 k_M}{4}(\mu_1 + \mu_2) \right] |\zeta_1|^2 + \frac{\gamma_1 k_M}{4} \left[\frac{|e_i|^2}{\mu_2} + \frac{4|i^*|^2}{\mu_1} \right] |e_i|^2 \end{aligned}$$

and we see that for sufficiently small values of μ_1 and μ_2 the factor of $-|\zeta_1|^2$ is positive, say actually not smaller than $q_m/2$. Thus, in view of (24) and $-\zeta_1^\top Q_2 \zeta_1 \leq -(1/2)\varepsilon_1(b-1)e_\omega^2$,

$$\dot{V}_1 + \dot{V}_2 \leq -\frac{q_m}{2} |\zeta_1|^2 - \frac{[R + k_{px}']}{l_M} |e_i|^2 - \frac{1}{2} \left[\varepsilon_1(b-1) - \frac{k_M}{l_m} - 1 \right] e_\omega^2 \tag{26}$$

in which the factor of e_ω^2 is positive for sufficiently large b. Moreover, in view of the positivity of P, for appropriate (large) values of the control gains a, b, k_p, k_d, k_{px} and small values of k_i, ε_1 and ε_2 there exist positive constants q_1, q_2, q_3 such that (see the appendix for details)

$$q_1\left(|e_i|^2+|\zeta_1|^2\right)\leq V_1(\zeta_1)+V_2(e_i)\leq q_2\left(|e_i|^2+|\zeta_1|^2\right)$$
$$\dot V_1(\zeta_1)+\dot V_2(e_i)\leq -q_3\left(|e_i|^2+|\zeta_1|^2\right).$$

Global exponential stability of the origin follows.

IV. Simulation results

In the previous section we establish global exponential stability for the system in closed loop with the controller (20). This is a strong stability property since it implies robustness with respect to perturbations with arbitrarily large initial tracking errors. However, the theoretical contribution comes at the expense of high-order nonlinear gains –see (24) which in turn, is likely to cause large control values u. Other causes of large voltage inputs are clear from formula (20); notice that $\dot\omega^*$ is used in T_d and $\ddot\omega^*$ enters in u through the expression β_j –see (19c). In addition to this, the nature of the switched-reluctance motor which imposes the use of the sharing-torque technique, induces discontinuous switches in the expression of i^* –note that α_j may be considerably large in the neighborhood of $\{K_j(\theta)=0\}$.

Thus, in order to implement the controller (20) with reasonable control inputs some precautions must be taken. Firstly, a smooth reference velocity is to be preferred even if stability is guaranteed for piecewise differentiable reference trajectories. Hence, we mostly use a sequence of smoothened steps generated by

$$\omega^*(t)=\omega_0^*+\frac{(\omega_f^*-\omega_0^*)}{2}\big(1+\tanh(t-T)\big) \tag{27}$$

–see Figure 4 for an illustration and the definition of the different design parameters. Note that different reference

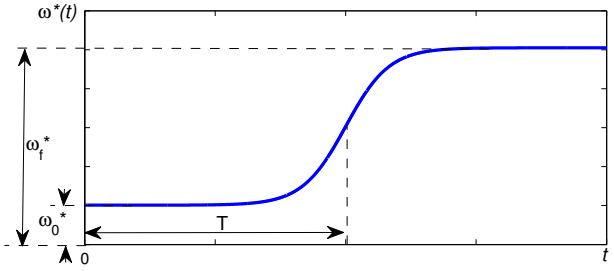

Fig. 4: Generic velocity reference profile constructed using hyperbolic tangent function

signals can be constructed by changing the numerical values of ω_0^*, ω_f^*, T and γ.

The functions m_j, which ensure the proper commutation of the motor, are defined via (8) where

$$m_j^+(\theta)=\begin{cases} f_j(q_{aj}) & 0<q_{aj}\leq\dfrac{\pi}{3N_r}\\ 1 & \dfrac{\pi}{3N_r}<q_{aj}\leq\dfrac{2\pi}{3N_r}\\ 1-f_j(q_{aj}) & \dfrac{2\pi}{3N_r}<q_{aj}\leq\dfrac{\pi}{N_r}\\ 0 & \text{otherwise}\end{cases} \tag{28}$$

$$m_j^-(\theta) = \begin{cases} f_j(q_{aj}) & \frac{\pi}{N_r} < q_{aj} \leq \frac{4\pi}{3N_r} \\ 1 & \frac{4\pi}{3N_r} < q_{aj} \leq \frac{5\pi}{3N_r} \\ 1 - f_j(q_{aj}) & \frac{5\pi}{3N_r} < q_{aj} \leq \frac{2\pi}{N_r} \\ 0 & \text{otherwise} \end{cases} \tag{29}$$

and

$$q_{aj} = \text{mod}\left(q, \frac{2\pi}{N_r}\right) + (j-1)\frac{2\pi}{N_r}. \tag{30}$$

Thirdly, it is customary to protect the motor to introduce input voltage saturation that is, using $\text{sat}_\delta(u_i)$ in place of u_i where $\text{sat}_\delta(u_i) = u_i$ if $|u_i| < \delta$ and $\text{sat}_\delta(u_i) = \delta \text{sgn} u_i$ otherwise.

Under the previous conditions we used SIMULINK™of MATLAB™to test the controller (15) on the *nonlinear* model (1), (2) with parameters borrowed from [9] and [14]: $R = 5$, $l_0 = 0.030H$, $l_1 = 0.020H$, $J = 0.001kg-m^2$, $\psi_s = 0.25$Wb and $N_r = 8$.

The controller gains are set to $k_{px} = 2000$, $a = 2580$, $b = 1900$, $k_d = 5050$, $k_i =$ 5e-4 and $k_p = 900$. Based on these values and the definitions of $K_j(\theta)$, $L_j(\theta)$, P and Q we have $k_M = 0.085$, $l_m = 0.01$, $l_M = 0.05$, $\gamma_1 = 105$ and $q_m =$ 1e-5 respectively then, the conditions for positive definiteness of P and Q are satisfied if $\mu_1 =$ 3e-6, $\mu_2 =$ 1e-6, $\varepsilon_1 = 0.04$ and $\varepsilon_2 =$ 1e-5.

For the sake of comparison, we present the results corresponding to two different runs of simulations: in the first case the control inputs are implemented without saturation, in the second case we set the saturation level to $\delta = 100$. The reference velocity consists in a smooth step as described above.

The simulation results are presented in Figs. 5–10. In Figs. 5, 6 and 9 are depicted, respectively, the current, the input voltages and the velocity tracking responses for the simulation test without input saturation. In Figs. 7, 8 and 10 we present the simulation results for the controller with an input saturation level of 100V. In both cases one may appreciate the fairly good performance; note the almost perfect velocity tracking albeit the slight increase of the response time, in the case that the inputs are saturated. Furthermore, the smaller plots in Figs. 5 and 7 show a zoom on the currents to appreciate the switching mechanism with hysteresis, employed to implement the virtual control input T_d.

V. CONCLUDING REMARKS

We have presented the first controller guaranteeing global exponential stability for switched-reluctance motors without velocity measurements. Our main result is a preliminary step towards the open problem of theoretically-validated global sensorless control for switched-reluctance motors. Current research is being carried out in this direction, in particular it focuses on the design of an angular-position observer to be implemented with a certainty-equivalence controller. Other significant problems under study include control under parametric uncertainty and control for the fully-nonlinear motor model (with inductances depending both on the angular position and the currents).

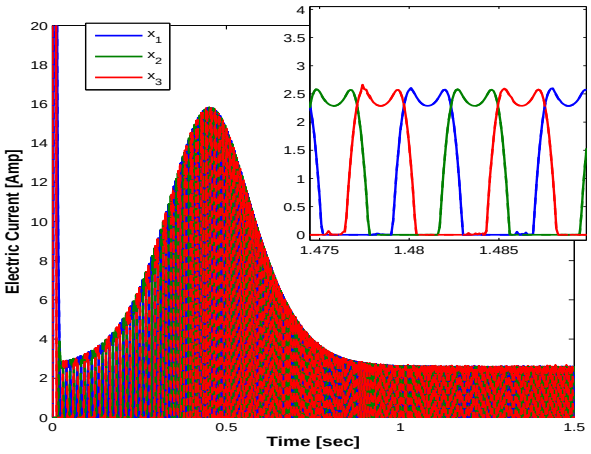

Fig. 5: Unsaturated controls: stator currents for the three phases and references

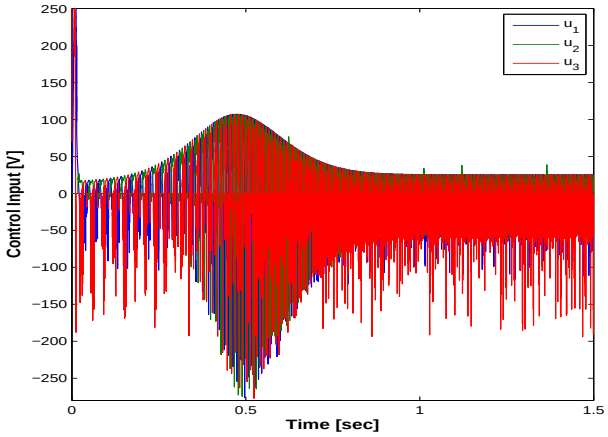

Fig. 6: Unsaturated controls: Input voltages

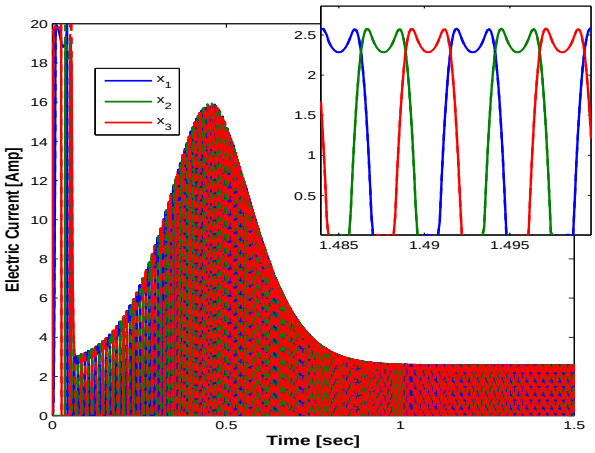

Fig. 7: Saturated controls (at 100V): stator currents for the three phases and references

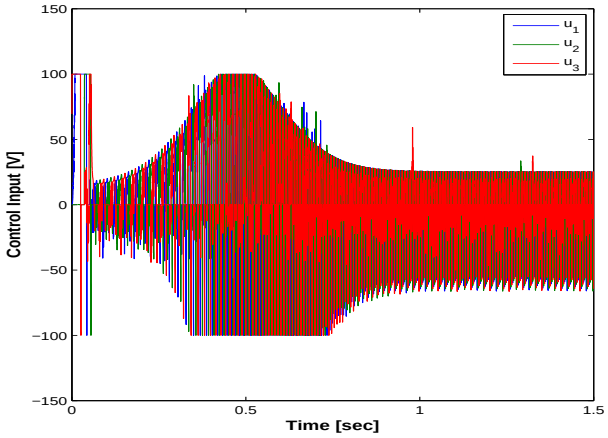

Fig. 8: Saturated controls (at 100V): Input voltages

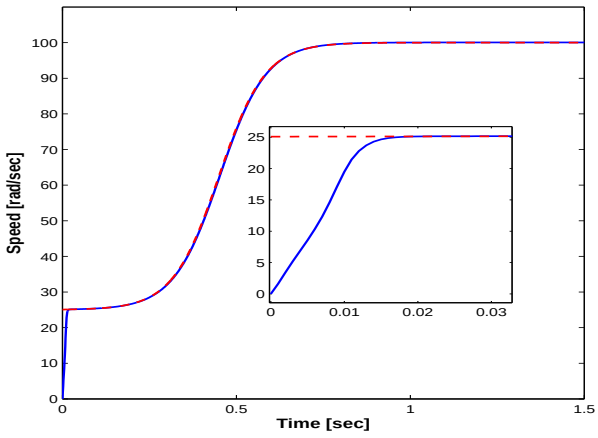

Fig. 9: Unsaturated controls: velocity tracking response

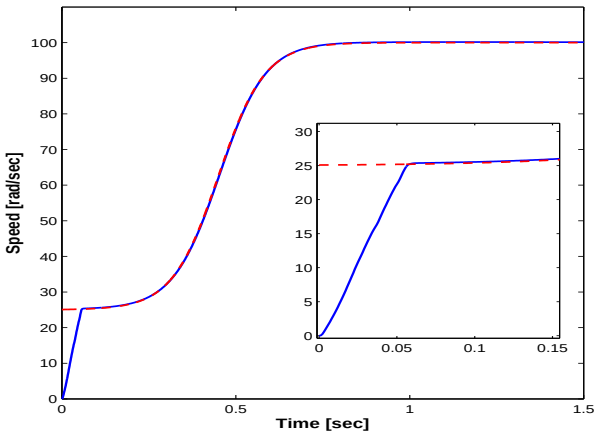

Fig. 10: Saturated controls (at 100V): velocity tracking response

Acknowledgements

The work of G. Espinosa is supported by DGAPA-UNAM under grant IN11121. This work was mostly carried out while A. Loria was visiting Facultad de Ingeniería - UNAM supported by Posgrado de Ingeniería - UNAM. A. Loría's and E. Chumacero's research leading to these results has also received funding from the European Union Seventh Framework Program [FP7/2007-2013] under grant agreement n°257462 HYCON2 Network of excellence. E. Chumacero benefits from a scholarship by CONACyT, Mexico.

REFERENCES

[1] G. LI, J. Ojeda, E. Hoang, M. Gabsi, and M. Lécrivain, "A new method of current density distribution for switching reluctance machine to increase average output torque," in *PCIM*, (Shanghai, China), 2009.

[2] J. Ojeda, X. Mininger, M. Gabsi, and M. Lécrivain, "Sinusoidal feeding for switched reluctance machine: Application to vibration damping," in *ICEM*, 2008.

[3] M. Rekik, M. Besbes, C. Marchand, B. Multon, S. Loudot, and D. Lhotellier, "Improvement in the field weakening performance of switched reluctance machine with continuous mode," *IET Electric Power Applications Journal*, no. 9, pp. 785–792, 2007.

[4] C. Hudson, N. Lobo, and R. Krishnan, "Sensorless control of single switch-based switched reluctance motor drive using neural network," *Industrial Electronics, IEEE Transactions on*, vol. 55, pp. 321 –329, jan. 2008.

[5] Y. Zheng, H. Sun, Y. Dong, and Z. Lei, "The research of stator current oriented method of switched reluctance motor," in *Control and Decision Conference, 2008. CCDC 2008. Chinese*, pp. 3184 –3188, july 2008.

[6] W. Xiaoyuan, P. Hao, and G. Zhi, "Double switch reluctance motors synchronization control system," in *Control and Decision Conference, 2008. CCDC 2008. Chinese*, pp. 3754 –3756, july 2008.

[7] H. Peyrl, G. Papafotiou, and M. Morari, "Model predictive torque control of a switched reluctance motor," in *Industrial Technology, 2009. ICIT 2009. IEEE International Conference on*, pp. 1 –6, feb. 2009.

[8] L. dos Reis, F. Sobreira, A. Coelho, O. Almeida, J. Campos, and S. Daher, "Identification and adaptive speed control for switched reluctance motor using DSP," in *Power Electronics Conference, 2009. COBEP '09. Brazilian*, pp. 836 –841, 27 2009-oct. 1 2009.

[9] G. Espinosa-Perez, P. Maya-Ortiz, M. Velasco-Villa, and H. Sira-Ramirez, "Passivity-based control of switched reluctance motors with nonlinear magnetic circuits," *Control Systems Technology, IEEE Transactions on*, vol. 12, pp. 439 – 448, may 2004.

[10] D. Taylor, "Pulse-width modulated control of electromechanical systems," *IEEE Trans. Automat. Contr.*, vol. AC-37, pp. 524–528, 1992.

[11] M. Feemster, P. Aquino, D. M. Dawson, and A. Behal, "Sensorless rotor velocity tracking control for induction motors," *IEEE Trans. Contr. Syst. Technol.*, vol. 9, no. 4, pp. 645–653, 2001. DOI: 10.1109/87.930976.

[12] A. Loria, G. Espinosa, and E. Chumacero, "Speed-sensorless control of switched-reluctance motors with uncertain payload," in *Proc. IEEE American Control Conference*, (Washington, D.C.), 2013. To appear.

[13] R. Ortega, A. Loría and R. Kelly, "A semiglobally stable output feedback PI2D regulator for robot manipulators," *IEEE Trans. on Automat. Contr.*, vol. 40, no. 8, pp. 1432–1436, 1995.

[14] M. Ilic-Spong, R. Marino, S. Peresada, and D. Taylor, "Feedback linearizing control of switched reluctance motors," *IEEE Trans. Automat. Contr.*, vol. AC-32, pp. 371–379, 1987.

[15] R. Ortega, A. Loría P. J. Nicklasson, and H. Sira-Ramírez, *Passivity-based Control of Euler-Lagrange Systems: Mechanical, Electrical and Electromechanical Applications*. Series Comunications and Control Engineering, Springer Verlag, London, 1998. ISBN 1-85233-016-3.

VI. APPENDIX

A. Positivity of Q

Positivity of Q_1

Claim 1: Given k'_p, k_d, k_i and a, b such that:

$$b \geq 2a + 1 \quad k'_p > k_d \tag{31}$$

then $\exists\ \varepsilon_1, \varepsilon_2 > 0$ s.t. $Q_1 \geq 0$

Proof of Claim 1. Let

$$\lambda = \frac{k_d}{k'_p} < 1, \tag{32}$$

$$\varepsilon_1 \leq \min\left\{1, \frac{k_d}{3b}, \frac{a\lambda}{2b(\lambda+1)}\right\}, \tag{33}$$

$$\lambda_2 := \frac{a}{\varepsilon_1 b} \tag{34}$$

and ε_2 be such that

$$\frac{\varepsilon_2}{\varepsilon_1} \leq \frac{1}{k_i}\min\Big\{\alpha_1, \alpha_2, \alpha_, \alpha_4\Big\} \tag{35}$$

where $\alpha_1 = k_d$, $\alpha_2 = \dfrac{(b-1-2a)}{2}$, $\alpha_3 = \dfrac{\varepsilon_1 a}{2}$ and $\alpha_4 = \dfrac{k_i}{k'_p}\left[1 + \dfrac{\lambda}{\lambda_2 - 1}\right]^{-1}$.

Note that given a, b, k'_p, k_i and k_d satisfying (31), the conditions (33) and (35) hold for sufficiently small values of ε_1 and ε_2. Also note that $\lambda_2 > 1$ since, in view of (33) we have $a > b\varepsilon_1$. We show that if (32)–(35) hold then Q_1 is diagonal dominant. It is so if the following hold

$$\varepsilon_1 \left|\lambda - 1\right| k'_p + \varepsilon_2 k_i \leq \varepsilon_1 k'_p \tag{36}$$

$$\varepsilon_2 k_i + \left|\varepsilon_2 k_i - \varepsilon_1 a\right| \leq \varepsilon_1(b-1) - \frac{2\varepsilon_2 k_i}{\varepsilon_1} \tag{37}$$

$$\varepsilon_1 k'_p \left|\lambda - 1\right| + \varepsilon_2 k_i + \varepsilon_1 a \leq \lambda k'_p\Big(\frac{a}{b} - \varepsilon_1\Big) \tag{38}$$

Since $\lambda < 1$ (36) holds if

$$\varepsilon_1 k'_p \geq \varepsilon_2 k_i + \varepsilon_1(1-\lambda)k'_p \quad \Leftrightarrow \quad \varepsilon_1 \lambda k'_p \geq \varepsilon_2 k_i$$

which is equivalent to

$$\frac{\varepsilon_2}{\varepsilon_1} \leq \frac{\lambda k'_p}{k_i} \tag{39}$$

which holds in view of (35) and (32).

Now, we show that (37) holds. Again, from (35) we have

$$\frac{\varepsilon_2}{\varepsilon_1} \leq \frac{a\varepsilon_1}{2k_i} \quad \Leftrightarrow \quad 2\varepsilon_2 k_i \leq \varepsilon_1^2 a \tag{40}$$

hence, (37) holds if

$$\varepsilon_1(b-1) - \varepsilon_1 a \geq 2\varepsilon_2 k_i + \varepsilon_1 a$$

which is satisfied if

$$\varepsilon_1(b-1) \geq 2(\varepsilon_2 k_i + \varepsilon_1 a)$$

or equivalently if

$$b - 1 - 2a \geq \frac{2\varepsilon_2 k_i}{\varepsilon_1}$$

which in turn, holds in view of (35).

Finally, we show that inequality (38) holds. Indeed since $\lambda < 1$, (38) is implied by

$$\frac{\lambda k_p' a}{b} \geq \varepsilon_1 k_p' + \varepsilon_2 k_i + \varepsilon_1 a + \lambda k_p' \varepsilon_1$$

which holds if

$$\frac{\lambda a}{2b} \geq \varepsilon_1 (1+\lambda) \tag{41}$$

and

$$\frac{\lambda k_p' a}{2b} \geq \varepsilon_2 k_i + \varepsilon_1 a. \tag{42}$$

Inequality (41) holds in view of (33) and since $2\varepsilon_2 k_i \leq \varepsilon_1^2 a$. Inequality (42) holds if

$$\frac{\lambda k_p' a}{2b} \geq \varepsilon_1 \Big(\frac{a\varepsilon_1}{2} + a \Big) \Leftrightarrow \frac{\lambda k_p'}{2b} \geq \Big(\frac{\varepsilon_1^2}{2} + \varepsilon_1 \Big).$$

Since $\varepsilon_1 < 1$, the latter holds if

$$\frac{\lambda k_p'}{2b} \geq \frac{3\varepsilon_1}{2} \quad \Leftrightarrow \quad \frac{k_d}{3b} \geq \varepsilon_1$$

which holds in view of (33).

Positivity of Q_2

Define $\eta := (1/2)\varepsilon_1(b-1)$ and $Q_2' := \text{diag}\{[0 \ \eta \ 0 \ 0]\}$ then, $\zeta_1^\top Q_2 \zeta_1 = \zeta_1^\top [Q_2 - Q_2'] \zeta_1 + (1/2)\varepsilon_1 (b-1) e_\omega^2$. The Schur Complement of $[Q_2 - Q_2']$ is non-negative if

$$\varepsilon_2 \geq \begin{bmatrix} -\varepsilon_2 k_p' \\ -k_d \varepsilon_2 \end{bmatrix}^\top \begin{bmatrix} \varepsilon_1 k_p' & 0 \\ 0 & k_d \big(\frac{a}{b} - \varepsilon_1 \big) \end{bmatrix}^{-1} \begin{bmatrix} -\varepsilon_2 k_p' \\ -k_d \varepsilon_2 \end{bmatrix}$$

the latter is equivalent to

$$\varepsilon_2 \geq \frac{\varepsilon_2^2 k_p'}{\varepsilon_1} + \frac{\varepsilon_2^2 k_p' \lambda}{\Big(\frac{a}{b} - \varepsilon_1 \Big)} \tag{43}$$

using $\lambda_2 := \dfrac{a}{b\varepsilon_1}$ we see that (43) holds if

$$\varepsilon_2 \geq \frac{\varepsilon_2^2 k_p'}{\varepsilon_1} + \frac{\varepsilon_2^2 k_p' \lambda}{(\lambda_2 - 1)\varepsilon_1} = \frac{\varepsilon_2^2 k_p'}{\varepsilon_1} \Big[1 + \frac{\lambda}{\lambda_2 - 1} \Big]$$

which holds in view of (35).

B. Negativity of $\dot{V}$

We establish that the factor of e_ω^2 in (26) may be rendered positive. From (22) and (23) we see that the argument of $\min\{\cdot\}$ in (33) equals $k_d/3b$. Therefore, ε_1 must belong to the interval

$$\Big[\frac{c}{b-1}, \quad \frac{k_d}{3b} \Big]$$

which is non-empty in view of (22).